LB-SCAM: A learning-based method for efficient large-scale sensitivity analysis and tuning of single column atmosphere model (SCAM)

Jiaxu Guo[1,8], Juepeng Zheng[2], Yidan Xu[6], Haohuan Fu[3,8], Wei Xue[4,8], Lanning Wang[5,8], Lin Gan[4,8], Ping Gao[4,8], Wubing Wan[4,8], Xianwei Wu[1,8], Zhitao Zhang[7], Liang Hu[1], Gaochao Xu[1], and Xilong Che[1]

[1]College of Computer Science and Technology, Jilin University, Changchun, China
[2]School of Artificial Intelligence, Sun Yat-sen University, Zhuhai, China
[3]Department of Earth System Science, Ministry of Education Key Laboratory for Earth System Modeling, Tsinghua University, Beijing, China
[4]Department of Computer Science and Technology, Tsinghua University, Beijing, China
[5]College of Global Change and Earth System Science, Beijing Normal University, Beijing, China
[6]National Meteorological Information Center, Beijing, China
[7]College of Geoexploration Science and Technology, Jilin University, Changchun, China
[8]National Supercomputing Center in Wuxi, Wuxi, China

Correspondence: Juepeng Zheng (zhengjp8@mail.sysu.edu.cn), Ping Gao (qdgaoping@gmail.com), Liang Hu (hul@jlu.edu.cn), and Xilong Che (chexilong@jlu.edu.cn)

Abstract. The single column model, with its advantages of low computational cost and fast execution speed, can assist users in gaining a more intuitive understanding of the impact of parameters on the simulated results of climate models. It plays a crucial role in the study of parameterization schemes, allowing for a more direct exploration of the influence of parameters on climate model simulations. In this paper, we employed various methods to conduct sensitivity analysis on the 11 parameters of the Single Column Atmosphere Model (SCAM). We explored their impact on output variables such as precipitation, temperature, humidity, cloud cover, among others, across five test cases. To further expedite experimentation, we utilized machine learning methods to train surrogate models for the aforementioned cases. Additionally, three-parameter joint perturbation experiments were conducted based on these surrogate models to validate the combined parameter effects on the results. Subsequently, targeting the sensitive parameter combinations identified from the aforementioned experiments, we further conducted parameter tuning for the corresponding test cases to minimize the discrepancy between the results of SCAM and observational data. Our proposed method can not only enhances the model performance but also expedites the speed of parameter adjustment, demonstrating good generality at the same time.

1 Introduction

Earth System Models (ESMs) are important tools to help people recognize and understand the effects of global climate change. Community Earth System Model (CESM) is one of the most popular and widely used ESMs, which includes atmosphere, ocean, land, and other components (Hurrell et al., 2013). Of these components, the Community Atmosphere Model (CAM)

(Neale et al., 2010; Zhang et al., 2018), plays an important role as the atmosphere component of CESM. Most of the physics parts in CAM are described as parameterization schemes with tunable parameters that are often derived from limited measurements or theoretical assumptions. However, since CAM needs to simulate all the grids, it takes a long time and a large amount of resources to run. Thus, Single Column Atmosphere Model (SCAM) (Bogenschutz et al., 2013; Gettelman et al., 2019) has been developed as a cheaper and more efficient alternative model for the purpose of tuning physics parameters (Bogenschutz et al., 2020). And in order to tune the parameters, we often need to conduct a large number of simulated experiments. This will result in significant computational costs. Meanwhile, SCAM only needs to simulate one single column, and only one process is required for each run of one case to complete the simulation. As a result, SCAM becomes a natural tool for studying how the parameters would affect the uncertainty in the modeling results, and the use of SCAM for large-scale experiments is more practicable due to its advantage of lower requirements for computing resources.

Climate models are among some of the most complex models, for a model, we can abstract it as a function with numerous independent and dependent variables, and there exists uncertainty between them. In research, identifying independent variables that significantly affect the dependent variable can help to quickly understand the relationship between them. Sensitivity analysis (SA) is an important method used to achieve this purpose. (Saltelli et al., 2010). A rich set of numerical and statistical methods have been developed over the years to study the uncertainty in models in many different domains, ranging from natural sciences, to engineering, and risk management in finance and social sciences (Saltelli et al., 2008). SA of climate models generally involves two steps: generating representative samples with different values of parameters using a specific sampling method; and explore and identify the sensitivity metrics between the model output and the parameters to study. Typical approaches include: the Morris One-At-a-Time (MOAT) method that uses the Morris sampling scheme (Morris, 1991), which generates samples uniformly and has a good compute efficiency, and the variance-based Sobol method generally requires a lot more samples to achieve a good coverage of the space (Sobol', 1967; Saltelli, 2002). Other similar ideas to achieve a good representation of the sample space with a quasi-random sequence include the quasi-Monte Carlo (QMC) (Caflisch, 1998) and the Latin hypercube (LHC) (McKay et al., 2000) sampling methods. The samples obtained from these sampling methods can be combined with sensitivity analysis methods such as Sobol(Sobol', 1967), High-dimensional model representation (HDMR, Li et al. (2010)), Random balance designs fourier amplitude sensitivity test (RBD-FAST, Goffart et al. (2015)), Delta moment-independent measure (Plischke et al., 2013), etc. This allows for an assessment of the individual parameter impacts on global outcomes, as well as the interrelationships between pairs, i.e., second-order sensitivity.

However, in practical applications, the number of parameters we need to adjust is often more than two. When adjusting more parameters, considering the intricate connections between them, there will inevitably be mutual influences. Just like the three-body problem in astronomy, when simultaneously adjusting three or more parameters, the complexity will be much greater than adjusting each of these three parameters individually. Therefore, whether the sensitivity analysis results obtained based on existing methods can accurately provide us with the optimal combination of multiple parameters is a question worth considering. Therefore, investigating the overall impact of combined parameters on the system output is worthy of further exploration. This holds true for climate models as well.

After we have determined the combination of parameters to be tuned, we can then tune them to improve the performance of the model. With a general goal to achieve modeling results as close to the observations as possible, we can apply different optimization methods, such as the Genetic algorithm (GE) (Mitchell, 1996), Differential Evolution (DE) (Storn and Price, 1997), Particle Swarm Optimization (PSO) (Kennedy and Eberhart, 2002), etc., to identify the most suitable set of parameters.

Continuous efforts have been put into the tunable parameters in climate models, especially for the their physics parameterization schemes (Yang et al., 2013; Guo et al., 2015; Pathak et al., 2021). Yang et al. (2013) analysed the sensitivity of nine parameters in the ZM deep convection scenario for CAM5 and used the Simulated Stochastic Approximation Annealing method to optimize the precipitation performance in different regions by zoning. Zou et al. (2014) conducted a sensitivity analysis for seven parameters in the MIT-Emanuel cumulus parameterization scheme in RegCM3. The precipitation optimization process for the CORDEX East Asia domain was carried out using the Multiple Very Fast Simulated Annealing method.

For all the stages mentioned above, the compute cost of running the model become a major constraining factor that stop us from exploring more samples and identifying more optimal solutions. People sometimes use surrogates (such as the generalized linear model (GLM) (Nelder and Wedderburn, 1972)) instead of the actual model to further reduce the compute cost. For example, the study of the sensitivity of simulated shallow cumulus and stratocumulus clouds to the tunable parameters of the subnormal uniform cloud layer (CLUBB) (Guo et al., 2015) investigated the sensitivity of 16 specific parameters, using the QMC sampling method and GLM as a surrogate, with experiments on three different cases (BOMEX, RICO, and DYCOMS-II RF01). A key problem to consider for the SA stage is to achieve a balance between the accuracy and the economy of compute (Saltelli et al., 2008). Another study (Pathak et al., 2021) used the single-column case ARM97 to explore 8 parameters related to the cloud processes, with Sobol as the sampling method, and spectral projection (SP) and basis pursuit denoising (BPDN) as the surrogate model. In an ideal case, a more thorough study of the parameters that can provide more concrete guidance for the parameter selection, would require a joint SA and tuning of different single-column cases, as well as combinational study of the most sensitive parameters. There are toolkits such as PSUADE (Tong, 2016), DAKOTA (Dalbey et al., 2021) and STATA (Harada, 2012) that can implement SA and tuning. These software tools have made remarkable contributions to advancing the development of generic frameworks. However, with the progress of high-performance computing, usability and ease of deployment have become crucial aspects for existing application scenarios. Particularly, in recent years, rapid advancements in fields like machine learning have made it meaningful to leverage machine learning methods to accelerate research progress.

In this paper, to facilitate researchers to better utilize SCAM, and to support a more efficient and convenient parameter tuning for the physical schemes in SCAM, we propose a learning-based method, LB-SCAM for efficient large-scale SA and tuning. In summary, our proposed LB-SCAM mainly make the following contributions.

1. We selected 11 parameters from three different physical schemes in SCAM, sampled them within a certain range, and utilized machine learning methods to train surrogate models for the response of model outputs to parameter variations. We selected five typical cases from SCAM and trained individual surrogate models for each of them. This further enhances the efficiency of conducting large-scale parameter testing for SCAM.

Table 1. List of single column atmosphere model cases tested.

Case	Full name	Lat	Lon	Date	Type
ARM95	ARM Southern Great Plains	36	-97	July 1995	Land convection
ARM97	ARM Southern Great Plains	36	-97	June 1997	Land convection
GATEIII	GATE Phase III	9	-24	August 1974	Tropical convection
TOGAII	Tropical W. Pacific Convection	-12	131	December 1992	Tropical convection
TWP06	Tropical Ocean Global Atmosphere	-2	154	January 2006	Tropical convection

2. With the samples obtained in the previous step, we conducted sensitivity analyses using five typical sensitivity analysis methods to assess the impact of these 11 parameters on four output variables in SCAM. Meanwhile, based on the surrogate models trained in the previous step, we conducted single-parameter and three-parameter joint perturbation experiments separately. This allowed us to identify, for each case, the most sensitive combination of three parameters.

3. Building upon the first two steps, we further conducted a parameter optimization process for the mentioned cases and variables. Additionally, we delved deeper into the patterns observed in the total precipitation (PRECT) variable. This exploration included examining the distribution patterns in the three-dimensional parameter space and identifying different characteristics among the different cases.

Using our proposed LB-SCAM, we perform an extensive set of SA and tuning experiments for five cases of SCAM (both independently and jointly), targeting the precipitation performance. Besides SA analysis that provides sensitivity evaluation of each single parameter, we are also able to study the sensitivity of a combination of three, four or even five arbitrary parameters. At the tuning stage, our improved optimization scheme (targeting the same parameters) leads to 24.4% more accurate output of precipitation compared to control experiments, with a more than 50% saving in compute cost compared to using only the optimization algorithm.

2 Enabling a workflow of SA and parameter tuning

2.1 Model description

This paper focuses on the single column model of the atmosphere model CAM5, i.e. SCAM5 (Bogenschutz et al., 2012), extracted from CESM version 1.2.2, one of the two versions that are efficiently supported on the Sunway TaihuLight Supercomputer (Fu et al., 2016). Our research of this paper is mainly based on five typical cases in SCAM5, as shown in Table 1. Among the five cases, two cases are located in the Southern Great Plains, which mainly study land convection. The other three cases are located in the tropics and mainly study tropical convection (Thompson et al., 1979; Webster and Lukas, 1992; May et al., 2008).

Table 2. Observed variables included in the IOP file of each case.

Variable	Description	ARM95	ARM97	GATEIII	TOGAII	TWP06
Prec	Precipitation rate	✓	✓	✓	✓	✓
totcld	Total cloud	✓	✓	-	-	✓
shflx	Surface sensible heat flux	✓	✓	-	✓	✓
lhflx	Surface latent heat flux	✓	✓	-	✓	✓
U	Eastward wind speed	✓	✓	✓	✓	✓
V	Northward wind speed	✓	✓	✓	✓	✓
Q	W.V. Mixing Ratio	✓	✓	✓	✓	✓
T	Temperature	✓	✓	✓	✓	✓
omega	vertical motion	✓	✓	✓	✓	✓
windsrf	Surface wind speed	✓	✓	-	✓	✓
REHUM	Relative humidity	-	-	✓	-	✓
CAPE	Convective available potential energy	-	-	✓	-	-

Table 3. Output variables studied in this paper and their meanings.

Variable	Description
PRECT	Total (convective and large-scale) precipitation rate (liq + ice)
CLDTOT	Vertically-integrated total cloud
Q850	Specific Humidity at 850 mbar pressure surface
T850	Temperature at 850 mbar pressure surface

As shown in Table 23, the number of observations included in the IOP (Intensive Observation Periods, Gettelman et al. (2019)) file varies from case to case. In order to explore a joint parametric sensitivity analysis and tuning across all the five cases, we pick the intersection of the data owned by these cases, PRECT, Q850, T850 and CLDTOT as the main research subject. The parameters listed in Table 4 are the main study targets (Qian et al., 2015) in this paper and the ones tested in the workflow. The parameters are selected from the ZM deep convection scheme (Zhang, 1995), the UW shallow convection scheme (Park, 2014), and cloud fraction (Gettelman et al., 2008). In the experiments in this paper, the lower and upper bounds of each parameter are 50% and 150% of the default value, respectively. For parameters with physical constraints, such as cldfrc_rhminh and cldfrc_rhminl, the values are ratios, so they are not more than 1.

In the original version of SCAM, only some of the parameters to be studied are tunable, while the rest are hard-coded in the model. To improve the flexibility of the model so that the 11 parameters we want to study are tunable, we have modified the source code of the model, to support the tuning and study of a wider range of parameters. The corresponding Fortran source code, as well as the XML documentation are also modified accordingly.

Table 4. List of parameters in the framework that can be tuned and applied to the experiment.

Abbr.	Name	Description	Low Range	Default	High Range	Category
pz1	c0_lnd	Deep convection precipitation efficiency over land	0.00295	0.0059	0.00885	ZM Deep convection
pz2	c0_ocn	Deep convection precipitation efficiency over ocean	0.0225	0.045	0.0675	ZM Deep convection
pz3	ke	Evaporation efficiency of precipitation	5e-7	1e-6	1.5e-6	ZM Deep convection
pz4	tau	Time scale for consumption rate deep CAPE	1800	3600	5400	ZM Deep convection
pz5	capelmt	Threshold value for CAPE	35	70	105	ZM Deep convection
pz6	alfa	Maximum cloud downdraft mass flux fraction	0.05	0.1	0.15	ZM Deep convection
pu1	rpen	Penetrative updraft entrainment efficiency	2.5	5.0	7.5	UW Shallow convection
pu2	kevp	Evaporative efficiency	1e-6	2e-6	3e-6	UW Shallow convection
pu3	rkm	Updraft lateral mixing efficiency	7	14	21	UW Shallow convection
pc1	rhminh	Threshold relative humidity for stratiform high clouds	0.7	0.8	0.9	Cloud fraction
pc2	rhminl	Threshold relative humidity for stratiform low clouds	0.7975	0.8975	0.9975	Cloud fraction

2.2 The workflow of sampling, SA and parameter tuning

The submission of assignments and the collection of results are important issues when carrying out a large number of model experiments at the same time. Prior to conducting the experiments, the user is often presented with a broad set of boundaries of the parameters to be tuned, and the specific configuration of each experiment has to be decided in detail according to these ranges of values. After a large number of experiments have been completed, as the output of SCAM is stored in binary files in NetCDF format, the precipitation variables we want to study need to be extracted from a large number of output files in order to proceed to the next step. It is therefore necessary to provide the researcher with an automated experiment-diagnosis process. In general, which parameters to tune and how to tune them are questions that deserve our attention.

Based on the above needs, we have designed the SCAM parameter sampling, SA, tuning and analysis workflow. We integrate the collection and processing script for the post-sampling results. It supports a fully-automated parameter tuning and diagnostic analysis process, a large number of concurrent model tests, and the search for the best combination of parameter values for SCAM performance within a given parameter space. Also, with the help of the training surrogate model, more parameter fetches can be tested in less time. The simulation results of the real model will be used as validation. This will further accelerate the degree of automation of scientific workflows and thus accelerate the conduct of research in this area of the earth system models.

The overview of the whole scientific workflow is shown in Figure 1. In order to make full use of computing resources and complete the sampling process as soon as resources allow, the proposed method supports parallel sampling processes, as shown in Figure 2. Since SCAM is a single-process task and the computation time per execution is also short, it is feasible to execute a large batch of SCAM instances during the sampling stage.

Specifically for the application scenario in this paper, the execution process of the workflow is as follows.
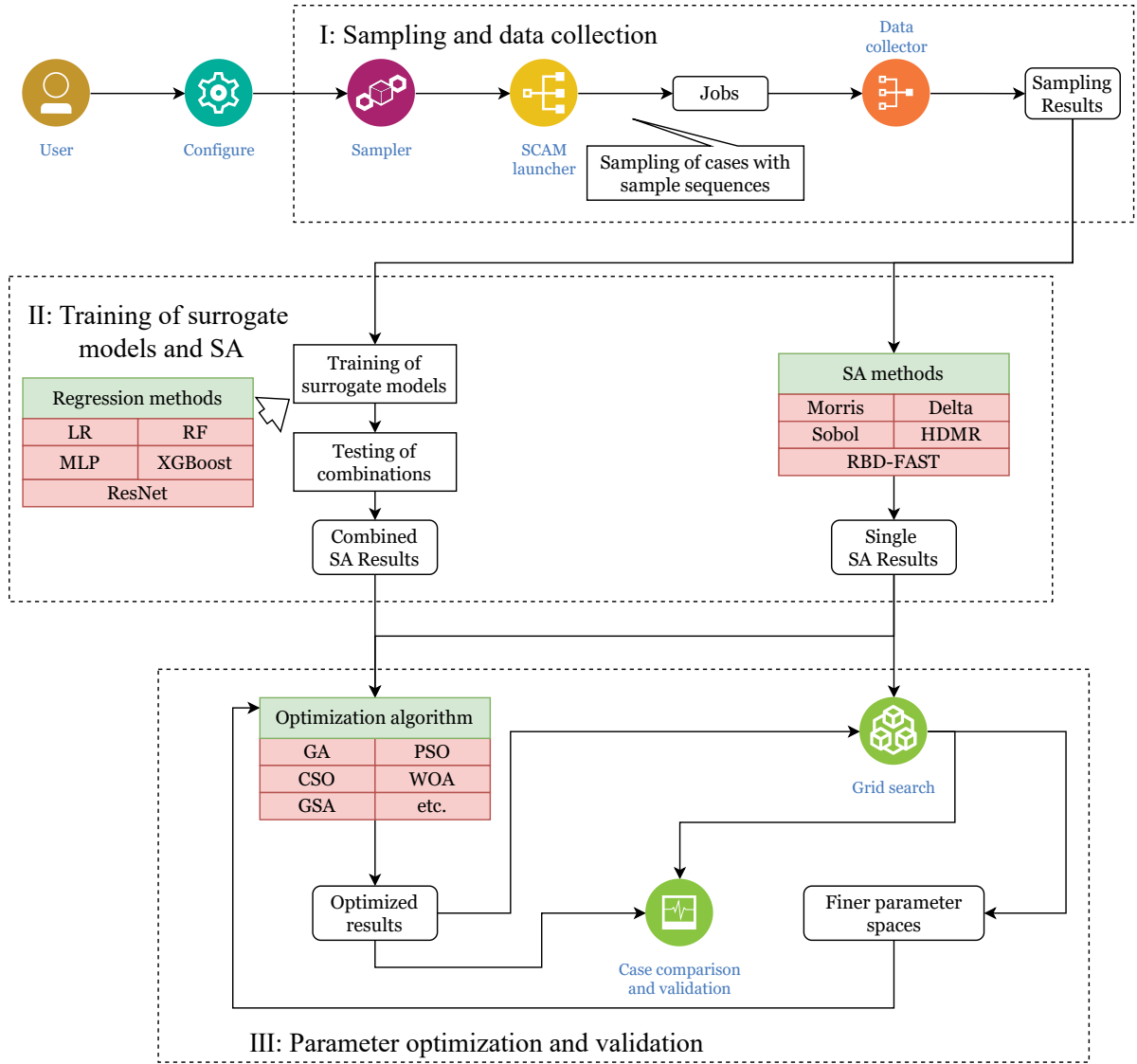
Figure 1. The overall workflow of the proposed method. Part I performs the sampling and the collection of results of parallel instances. Part II uses traditional SA methods to derive sensitivities of individual parameters, and at the same time, reuse the samples to derive learning-based surrogate models. Combining the surrogate models, we can then also perform joint sensitivity analysis of a set of parameters. Guided by the SA results from Part II, Part III performs parameter tuning, also with the surrogate models. SCAM launcher, the data collector and the jobs therein represent the batch execution of the SCAM algorithm, which is described in more detail in Figure 2.
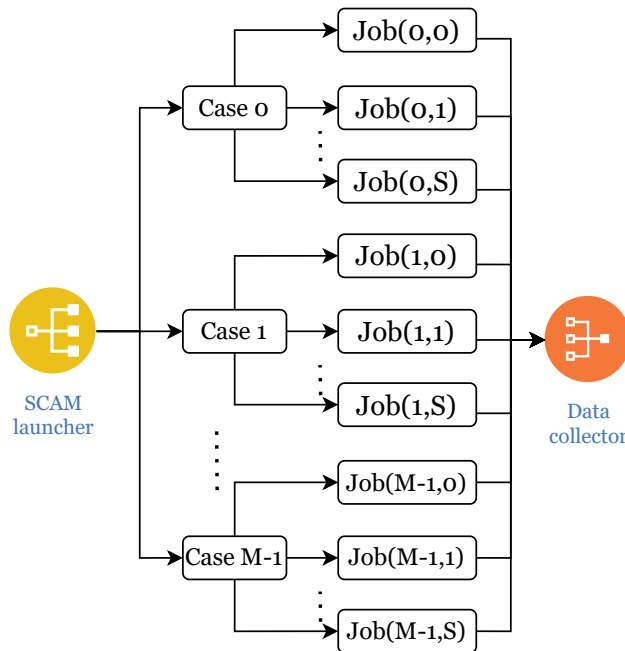
Figure 2. Detailed parallelism schematic when running a large number of instances of multiple cases simultaneously. In this process the required SCAM tasks are launched simultaneously by the launcher and the results of their runs are collected by the data collector.

1. Sampling and data collection (shown as Part I in Figure 1): In this part, our tool generates the sequence of samples to investigate in the sampling step. Our tool currently supports the Sobol sequence, which can later be used by the Sobol, Delta (Plischke et al., 2013), HDMR (Li et al., 2010), and RBD (Plischke et al., 2013) SA methods, and the Morris sampling sequence, which can later be used by the MOAT method (Morris, 1991). Users are suggested to adjust the size of the sequence according to the currently available computational resources. As the results of this step will be used as the training set for generating the surrogate model, users are encouraged to run a large batch when parallel resources are available, so as to improve the performance of the resulting surrogate model. The process of launching the parallel cases and collecting the results is handled by the SCAM launcher and collector.

2. Surrogate model training and sensitivity analysis (shown as Part II in Figure 1): Based on the sampling results from the Morris or the Sobol sequence, we integrate existing methods, such as MOAT, Sobol, Delta, HDMR, and RBD to achieve their individual evaluations of each single parameter's sensitivity, as well as a comparison result of these methods. We also use the sampling results of the Saltelli sequence and the Morris sequence, to train regression including neural network (NN) based surrogate models. In this section, different regression methods are used to compare their fits and the best fitting method to train the final surrogate model. With the efficiency to project a result in seconds rather than minutes, we can apply it for evaluation of sensitivities of a combination of multiple parameters.

3. Parameter tuning and validation (shown as Part III in Figure 1): With the NN-based surrogate model to cover expanded search space with less time, we also propose an optimization method that combines grid searches by the surrogate model, which achieves better results with less compute time. The results of parameter tuning are then validated through running of real SCAM models. In addition, at the very end, we perform a comparison on the optimization results between the joint optimization across five cases and the independent optimization of the five cases. Results demonstrate the different and the correlation of different cases, and the potential of performing grid-specific tuning in the future.

3 Methodology

3.1 Sampling of SCAM

As an important preprocedure, the sampling provides the basis for analysis of SA. It will generate a sequence of changing inputs and parameters to observe the corresponding change in the output. The different mathematical approach that we take to perform sampling would certainly affect the features that can be captured from the system.

In our proposed workflow, we integrate both Morris and Saltelli for the sampling step in our tuning workflow, as both of them are still used in many climate model related SA studies (Pathak et al., 2021). The Morris sampling drives the MOAT SA module afterwards, while the Saltelli sampling drives four different SA modules (Sobol, Delta, HDMR, and RBD-FAST) shown in Table 5.

After sampling, we will conduct a preliminary analysis of the sampled results to find out the proportion distribution in which the output results are better than the control trials under different values of each parameter. RMSE (Root mean square error) will be used to measure the error between the output and the observed values and is defined as follows.

$$RMSE = \sqrt{\frac{1}{N} \sum_{i=1}^{N} (y_i - \hat{y}_i)^2} \tag{1}$$

Where $\hat{y}_i$ is the output at the ith time step of the current sample, while y_i is the observation at the corresponding time step.

Table 5. SA methods integrated in the workflow and used as a cross-reference to the proposed method.

Name of method	Abbr.	Reference
Morris sensitivity analysis	Morris	Morris (1991)
Delta moment-independent measure	Delta	Plischke et al. (2013)
Sobol' sensitivity analysis	Sobol	Sobol (1993)
High-dimensional model representation	HDMR	Li et al. (2010)
Random balance designs fourier amplitude sensitivity test	RBD-FAST	Goffart et al. (2015)

3.2 Training a learning-based surrogate model

Surrogate models are an important tool to speed up our large-scale parametric experiments. It can replace the running process of the original model, thus saving computing resources. The essence of training surrogate models for SCAM is a regression analysis problem. In this paper, we introduce the following regression methods to generate surrogate models. These include Linear regression (LR,Yan et al. (2015)), but also ensemble learning methods such as Random forest (RF, Breiman (2001)) and eXtreme Gradient Boosting (XGBoost, XingFen et al. (2018)). Meanwhile, we also incorporate methods that use neural networks, such as Multilayer Perceptron (MLP, Tang et al. (2016)) and Residual Network (ResNet, He et al. (2016); Shi et al. (2022)).

In order to combine the various regression analysis methods described above, in this paper we design an adaptive scheme to determine the method that best captures the non-linear characteristics of the original model, and thus obtain the most appropriate surrogate model. To keep an acceptable level of accuracy of surrogate models, we choose to train respective models for each different SCAM case (the underlying assumption is that the model should learn the different patterns in different SCAM case locations). As the Saltelli sequence of samples have a good representation of the entire parameter space, we expect the model to perform generally well in different parameter combinations. In addition, for the hyper-parameters in the process of training the surrogate model, ablation experiments will also be performed to determine the most appropriate hyper-parameters, leading to better training.

3.3 Sensitivity analysis for a single parameter and combinations of parameters (enabled by the NN-based surrogate model)

The SA methods, similar to the climate model itself, have their corresponding uncertainties. The SA methods provide a best estimation of each parameter's sensitivity, according to their respective analytical principles. Therefore, each different method might have its advantages and disadvantages in different ranges of the parameter values.

As a result, in our workflow shown in Figure 1, we choose to integrate multiple SA methods, including the ones that can be built on the Sobol sequence, such as Delta, HDMR, and RBD-FAST, and the Morris method, which is still used often for climate models, due to its efficiency advantage. The integration of multiple methods enables us to better evaluate the uncertainty of different SA methods. As the sensitivity values calculated by the different methods are of different orders of magnitude, these sensitivities have been normalised using min-max method for comparison purposes.

The parameters may interact with each other, and the effects of multiple parameters on the simulation results may be superimposed. Therefore, tuning multiple parameters generally have a more significant effect than tuning a single parameter. With the help of commonly used sensitivity analysis methods mentioned above, it is easy to obtain the sensitivity of individual parameters. However, in cases where we need to identify and tune a set of parameters in a combined way, both the SA and the tuning task would involve a significantly improved level of compute resources.

An obvious benefit of using a surrogate model for training is that it is very fast to compute. Since the model has been trained, the time taken to output the surrogate results is much shorter. Therefore, we can try as many combinations of parameters as

possible with less computational resources. By applying the trained surrogate model, we will test the maximum fluctuation in the output of each case when the number of parameters adjusted at the same time is different. This will aid in our decision-making process to determine the scale of meaningful and beneficial large-scale multi-parameter perturbation tests.

The utilization of the learning-based surrogate model, on the other hand, provides a more feasible solution to this problem. Since the surrogate model has a very short running time and almost does not need to consider the problem of job queuing time, it makes it possible to complete a large scale parameter experiment in a short time.

3.4   Parameter tuning enhanced with NN-based surrogate model and grid search

After the most sensitive sets of parameters have been found, the stage of optimization will begin.

In the optimization stage, on the basis of combining the existing optimization algorithms (such as GA, PSO, WOA, etc.), we propose an enhanced optimization method based on grid search. By using grid search, the search scope can be further narrowed before and during the call to the existing optimization algorithm, so as to improve the efficiency of searching for better solutions. The process is as follows.

1. Determine the overall parameter space range for conducting the grid search based on the initial setup of the experiments.

2. The simulation output values corresponding to these grids are calculated in the surrogate model. Then the best performing points are selected and the new finer-grained search space is determined based on the aggregation of these points.

3. The optimization algorithm is carried out in the newly defined space and depending on the available computational resources it is decided whether SCAM is invoked to compute in each iteration round. Meanwhile, the final results will also be substituted into SCAM for verification.

4. If the same optimization result is obtained in three consecutive iterations, or less than a certain threshold of improvement compared to the last, the grid search operation of the first two steps is performed again, thus further reducing the search space, as can be seen from Algorithm 1. In this step, a new parameter space will be constructed with the position of the current best point at the centre and the distance of each parameter from the last best point as the radius.

5. After the refinement of the parameter search space, if the result remains the same, the optimization process can be considered to be over and SCAM can be run again using the derived parameters to verify the optimization results.

In Algorithm 1, Y_i is the value of the function in the ith iteration, ϵ is the threshold at which the results converge, p is the total number of parameters to be tuned, $x_{j,i}$ is the coordinates of x_j in the ith iteration, X_j denotes the maximum and minimum values initially set for x_j, and X_j^* denotes the maximum and minimum values of x_j in the upcoming grid search. Note that if one of these coordinates is outside the initial parameter space, the original parameter space boundary will be used as the new boundary.

Algorithm 1 Optimization process combined with grid search.
___

if $Y_i - Y_{i-1} < \epsilon$ **and** $Y_{i-1} - Y_{i-2} < \epsilon$ **then**

    for $j = 1$ **to** $j = p$ **do**

        if $x_{j,i} - |x_{j,i} - x_{j,i-3}| > X_{j,min}$ **then**

            $X^*_{j,min} = x_{j,i} - |x_{j,i} - x_{j,i-3}|$

        else

            $X^*_{j,min} = X_{j,min}$

        end if

        if $x_{j,i} + |x_{j,i} - x_{j,i-3}| < X_{j,max}$ **then**

            $X^*_{j,max} = x_{j,i} + |x_{j,i} - x_{j,i-3}|$

        else

            $X^*_{j,max} = X_{j,max}$

        end if

    end for

end if

Grid seach.

return $x_{j,i+1}$ **and** Y_{i+1}
___

3.5 Case correlation analysis based on Pearson correlation coefficient

235 Following the end of the tuning process, we further perform a comparison study among different cases, to derive valuable insights that would potentially lead to a physics module design that can accommodate the different features in different locations.

In our proposed method, the Pearson correlation coefficient method is used to measure the similarity between two cases (Schober et al., 2018). This coefficient is defined as the quotient of the covariance and standard deviation between two variables. By analyzing the similarity between the 'optimal' parameters of each case, these cases can be clustered. In this process, we

240 can explore whether for similar types of case, they may have similar responses to various parameters. This will also help us choose better parameter combinations when analyzing other cases, and even regional and global models, so as to achieve better simulations. The implementation is shown below.

1. Search the sensitive parameter sets for each output variable in each case.

2. For each case, the occurrence times of each parameter in the sensitive parameter combination are accumulated to obtain

245   a variable of M dimension, where M is the number of parameters. For example, for a combination of three parameters, the vector can be expressed as $(Value1, Value2, Value3)$.

3. The correlation between vectors of each case can be computed by the Pearson correlation coefficient method.

By the above procedure, we can obtain the similarity of the set of sensitive parameters among the cases. The correlation between different cases can also be analyzed for the case of finding the optimal values in the same parameter space. After each

250 case has found its optimal parameter values, this set of parameter values can also be represented by vectors. The same approach can be used to analyze the correlation between these vectors.

4 Experiments

4.1 Sampling of the SCAM cases

As mentioned earlier, the sampling scheme, which determines the set of points to represent the entire parameter space, is of
255 essential importance for the following sensitivity analysis and parameter tuning steps. Considering the compatibility between the sampling methods and the SA methods, our platform includes both the Morris (driving the MOAT SA method) and the Sobol sampling scheme (driving the Sobol, Delta, HDMR, and RBD-FAST SA methods). We use a total of 7,680 samples, with 1,536 samples for each of the five SCAM case. Of these, half (i.e. 768 samples) are used for MOAT, while the remaining half are used for the Sobol sequence. In this part of the experiment, we use the job parallelism mechanism mentioned earlier in
260 the text to execute these sample cases.

In our sampling, SA, and tuning study, we focus on the total precipitation output (PRECT). Figure 3 reflects the proportion of PRECT that outperforms the control experiments when each parameter is tuned from low to high in the range of values taken. From the results, we can see that for different cases there are differences in their response to parameter changes. Of particular interest is the distribution of pz4(tau). We can clearly see that for GATEIII, when the value of tau is small, there are
265 more good outputs; However, for the other cases, it is that when the value of tau is large, there are more outputs that perform well. It can also be seen from the proportion that tuning tau can lead to more good outputs. This is also in line with the results of our later experiments.

To further verify the conclusions here, we performed a single-parameter perturbation test on tau while keeping the other parameters as default values.

270 ### 4.2 Training learning-based models for parameter tuning

After obtaining the sampling results, we can train the surrogate model for each of the five cases using the method presented in Section 3.2. The samples generated by the two sampling methods are combined to form the dataset on which we train our surrogate model. In other words, each case has 1536 samples, and all cases have a total of 7680 samples to participate in the training. We split the training and test set in an 8:2 ratio and use RMSE as the loss function during training.
275 We trained surrogate models using five regression methods and used RMSE as a loss function to measure the training error. A comparison of the various methods is shown in Table 6. It can be seen that ResNet has the best performance on the five cases, and its error on the test set is lower than that of the other methods. Therefore, we will use the surrogate model trained by ResNet-18 for the following experiments. For the hyper-parameters in training using ResNet-18, we also conduct ablation experiments to achieve better training results. The results of the ablation experiment indicate that using a learning rate of 0.01
280 and a batch size of 32 is appropriate.
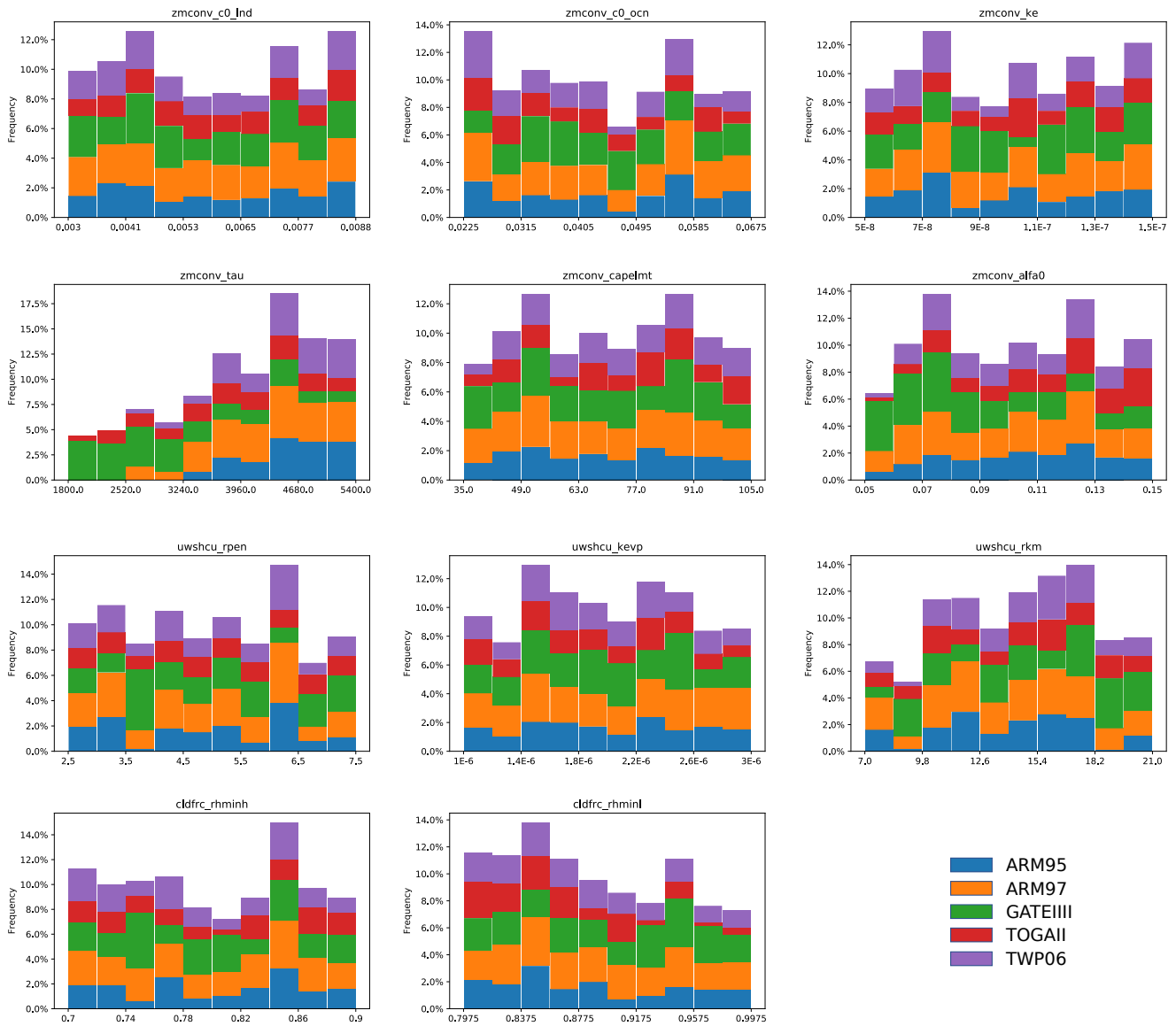
Figure 3. The proportion of sampled results where the output is better than the control experiments (i.e. experiments using default values). The x-axis shows the range of values for each parameter.

Table 6. Comparison of errors during training using various methods. RMSE is used as the loss function. The errors are from test sets.

Case	LR	RF	MLP	XGBoost	ResNet-18
ARM95	0.235	0.197	0.751	0.184	**0.172**
ARM97	0.188	0.158	0.555	0.136	**0.121**
GATEIII	0.646	0.432	1.335	0.538	**0.396**
TOGAII	0.179	0.112	0.223	0.118	**0.107**
TWP06	0.344	0.220	0.594	0.220	**0.203**

4.3 Single-parameter sensitivity analysis across different cases

After sampling, five SA methods listed in Table 5 are used to compute the sensitivity of these parameters to the PRECT, Q850, T850 and CLDTOT output. In addition, for the surrogate models we trained, we also adopted the single-parameter perturbation method to test their sensitivities. Heat maps are used to characterize the sensitivities of each parameter. As can be seen from Figure 4, there are differences in the results obtained from different SA methods.
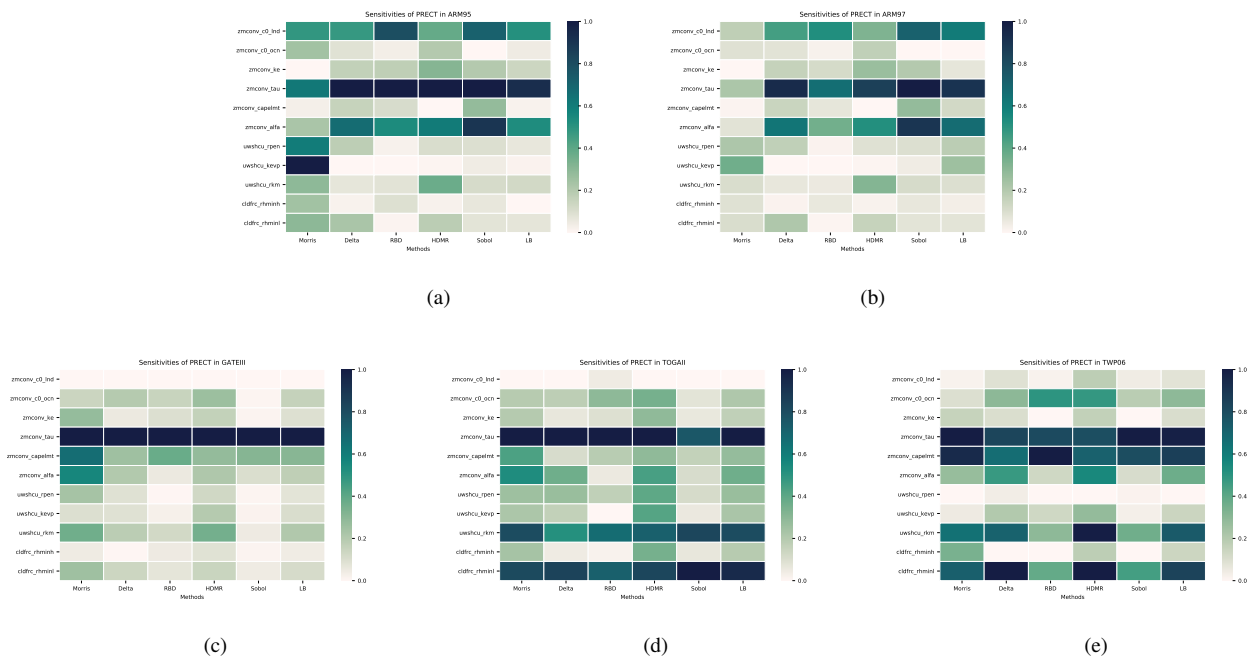
Figure 4. The comparison of the sensitivity of each parameter to PRECT comes from different analysis methods (including our proposed LB-SCAM) in five cases. Sensitivity results were normalised. (a)ARM95, (b)ARM97, (c)GATEIII, (d)TOGAII, (e)TWP06. The qualitative and quantitative similarities and differences in the sensitivity of each case to each parameter are reflected.

From the results of PRECT, it can be seen that the response of ARM95 and ARM97 to each parameter is basically the same, only a few quantitative differences exist in parameters such as zmconv_alfa, uwshcu_kevp and so on. Moreover, both cases are sensitive to zmconv_tau, which significantly outweighs the other parameters. For GATEIII, we can see that zmconv_tau similarly has a significant influence on it, but zmconv_alfa and uwshcu_rkm also have a large influence. In addition, the two SA methods of Morris and Sobol simultaneously show that cldfrc_rhminl also has a non-small effect. For TOGAII, it is interesting to find that zmconv_tau and cldfrc_rhminl have similarly significant effects. However, tau still has a far greater influence than other parameters on TWP06, which is similar to ARM95/97. Furthermore, the impact of zmconv_c0_ocn on this case is also notable. This clearly demonstrates that cases located in different locations exhibit varied responses to parameters. To sum up, zmconv_tau has a very significant significance for all cases.

We also compared the differences between these SA methods. To demonstrate the applicability of using our learning-based surrogate model in the SA process, we also show the SA results by using our trained learning-based surrogate models. For comparison across different methods, the most sensitive parameter obtained by each method is tau, but there are differences in the sensitivity of other parameters to some extent. For example, Delta and HDMR yield slightly greater sensitivity for the other parameters. In addition, Morris concluded that the sensitivity of these parameters is significantly greater than that of the other methods, that is, the gap between tau and the other parameters is smaller. This may be related to the sampling method, as Morris needs to use a different sequence of samples.

As can be seen from Figure 5, for the humidity variable Q850, we can clearly see that all five cases are highly sensitive to the parameter zmconv_tau. In addition, the sensitivity of zmconv_alfa is also relatively high. The cases TOGAII/TWP06 exhibit higher sensitivity to zmconv_capelmt, while the other three cases show less pronounced sensitivity. In terms of sensitivity analysis methods, the HDMR method provides more balanced parameter sensitivities, and this is particularly evident in the TOGAII case.

As can be seen from Figure 6, for the temperature variable T850, we can observe some more interesting phenomena. In the ARM95 case, all methods except Morris consider cldfrc_rhminl as the most significant parameter influencing the results, while Morris concludes that uwshcu_kevp is the strongest, followed by uwshcu_rpen. In the ARM97 case, we find that each SA method identifies different most sensitive parameters, posing a new challenge for our next step in parameter optimization. For the remaining three cases, there is less controversy between different methods. In each case, uwshcu_rkm has overwhelming dominance, and in GATEIII and TOGAII, the impact of zmconv_tau is also considerable. For TOGAII, the sensitivity of zmconv_capelmt and alfa should not be overlooked.

For the total cloud amount CLDTOT, we can also observe interesting conclusions from Figure 7. For the ARM95/97 cases, the results from various methods are consistent: the parameters zmconv_c0_lnd, zmconv_tau, and zmconv_alfa have a significant impact on the results. This reflects the convergence of the two cases. In the case of TWP06, the most noticeable factors are uwshcu_rkm, followed by cldfrc_rhminl. The conclusions drawn by various methods remain consistent.
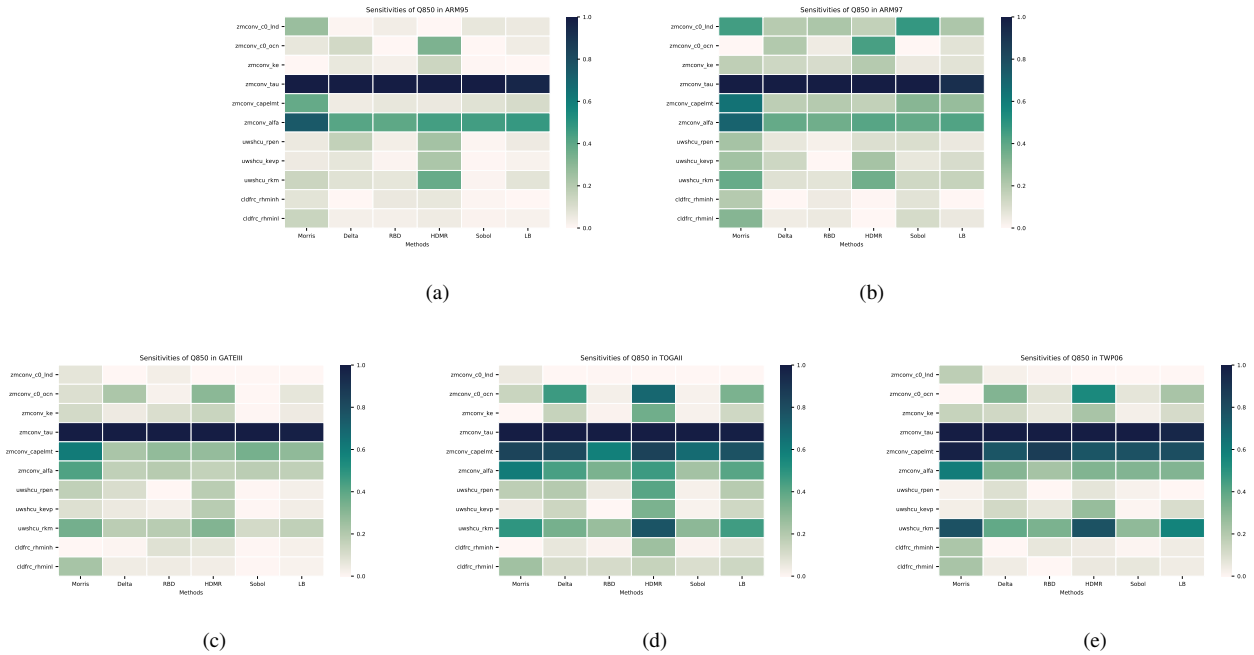
Figure 5. The comparison of the sensitivity of each parameter to Q850 comes from different analysis methods (including our proposed LB-SCAM) in five cases. Sensitivity results were normalised. (a)ARM95, (b)ARM97, (c)GATEIII, (d)TOGAII, (e)TWP06. The qualitative and quantitative similarities and differences in the sensitivity of each case to each parameter are reflected.

4.4 Joint multi parameter sensitivity analysis using learning-based surrogate models

As mentioned earlier, by using the learning-based surrogate models, we now have the capability to explore the sensitivity of
320 multi-parameter combinations. How many parameters is it reasonable to tune at the same time? Figure 8 illustrates the maximum PRECT output fluctuation that can be brought by different parameter combination sizes. As the number of parameters to be tuned simultaneously increases, the fluctuations that can be brought about are also greater. However, there is also a marginal effect as the number of parameters tuned simultaneously increases. We can see that when tuning four parameters, the gain effect on the result is already not significant. Therefore, considering the range of the most accurate parameter adjustment, we
325 limit the number of parameters adjusted simultaneously to three. In addition, we also note that for the ARM97 and TOGAII, their precipitation response for four parameters is even smaller than the response of the GATEIII for tuning one parameter. An important reason for this is that these two cases themselves have smaller precipitation values than GATEIII, whereas the Figure 8 uses the absolute values of precipitation.

As our study investigates 11 parameters related to the four variables, there are a total of 165 three-parameter combinations.
330 It would be difficult to test all these combinations using the original SCAM model, due to the high computational overhead. However, with the help of the surrogate model, we can instead accomplish these tests in less than a minute.
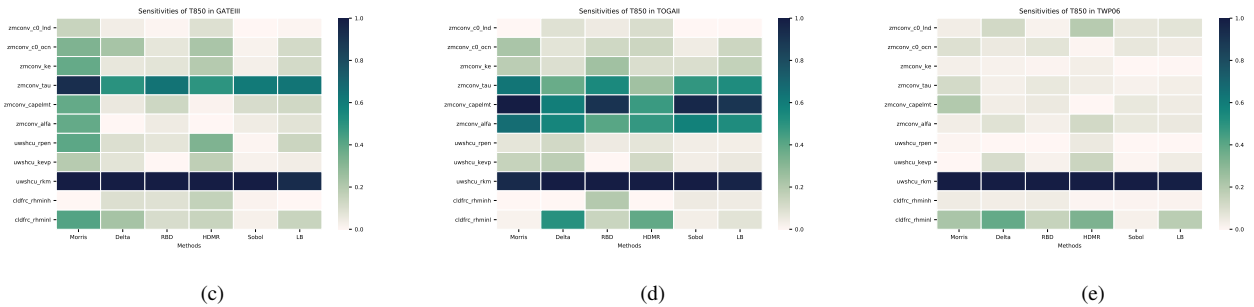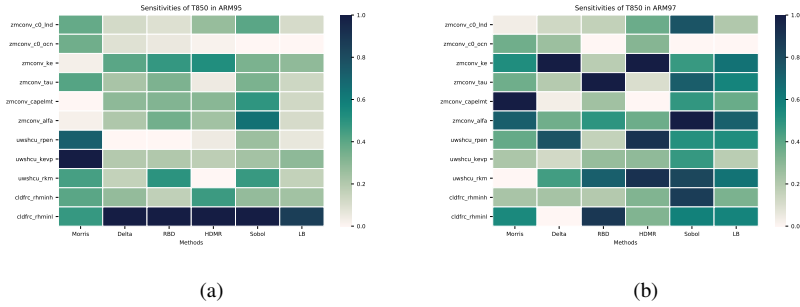
Figure 6. The comparison of the sensitivity of each parameter to T850 comes from different analysis methods (including our proposed LB-SCAM) in five cases. Sensitivity results were normalised. (a)ARM95, (b)ARM97, (c)GATEIII, (d)TOGAII, (e)TWP06. The qualitative and quantitative similarities and differences in the sensitivity of each case to each parameter are reflected.
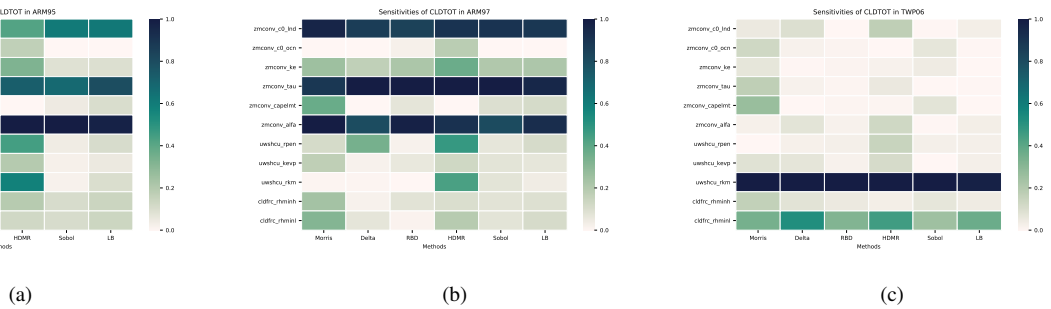
Figure 7. The comparison of the sensitivity of each parameter to CLDTOT comes from different analysis methods (including our proposed LB-SCAM) in five cases. (a)ARM95, (b)ARM97, (c)TWP06. The qualitative and quantitative similarities and differences in the sensitivity of each case to each parameter are reflected.
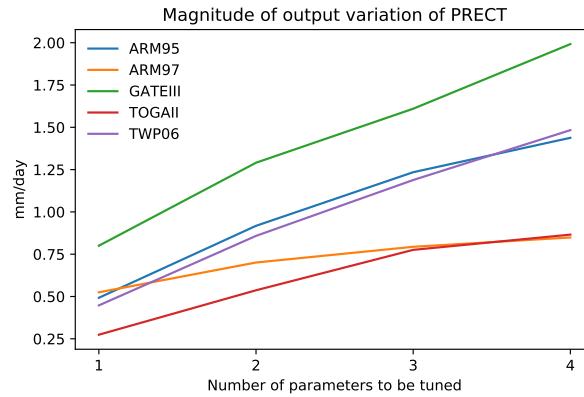
Figure 8. The maximum fluctuation in the output of each case when perturbing one to four parameters. The Y-axis represents the largest gap between the maximum and minimum values of precipitation output that can occur during the simulation period.

These combinations are listed in Table 7. Whale optimization algorithm(WOA, Mirjalili and Lewis (2016)) has been chosen as the method in this stage. RMSE is also selected as the metric of optimization effect. Next, we will explore further the sensitive parameter combinations.

Table 7. The most sensitive parameter combinations of each output variable.

Variables	ARM95	ARM97	GATEIII	TOGAII	TWP06
PRECT	pz1, pz4, pz6	pz1, pz4, pz6	pz4, pz5, pu3	pz4, pu3, pc2	pz4, pz5, pc2
Q850	pz4, pz5, pz6	pz4, pz5, pz6	pz4, pz5, pz6	pz4, pz5, pu3	pz4, pz5, pu3
T850	pz3, pu2, pc2	pz3, pz6, pc2	pz4, pu3, pc2	pz5, pz6, pu3	pz5, pu3, pc2
CLDTOT	pz1, pz4, pz6	pz1, pz4, pz6			pz6, pu3, pc2

4.5 Joint optimization for SCAM cases combined with grid search and learning-based models

335

Consequently, experiments combining the grid search and optimization algorithms will be performed. As above, WOA is still used as the optimization algorithm for this stage. To verify the correctness of the surrogate model, we also compare its output with SCAM.

For the effectiveness of the parameter tuning, the output after tuning is compared with the output of the control experiment

340 (i.e. before tuning) and the observed data after the individual cases had been tuned, as shown in Figure 9. Here, the experiments with the best optimization results are chosen for comparison. It is easy to see that in the control experiment there are several spikes where the simulated output is significantly higher than the observed values, as is the case in the first four cases. This is to say that these time steps, where the output is significantly larger than the observation in the control trial, are reduced after
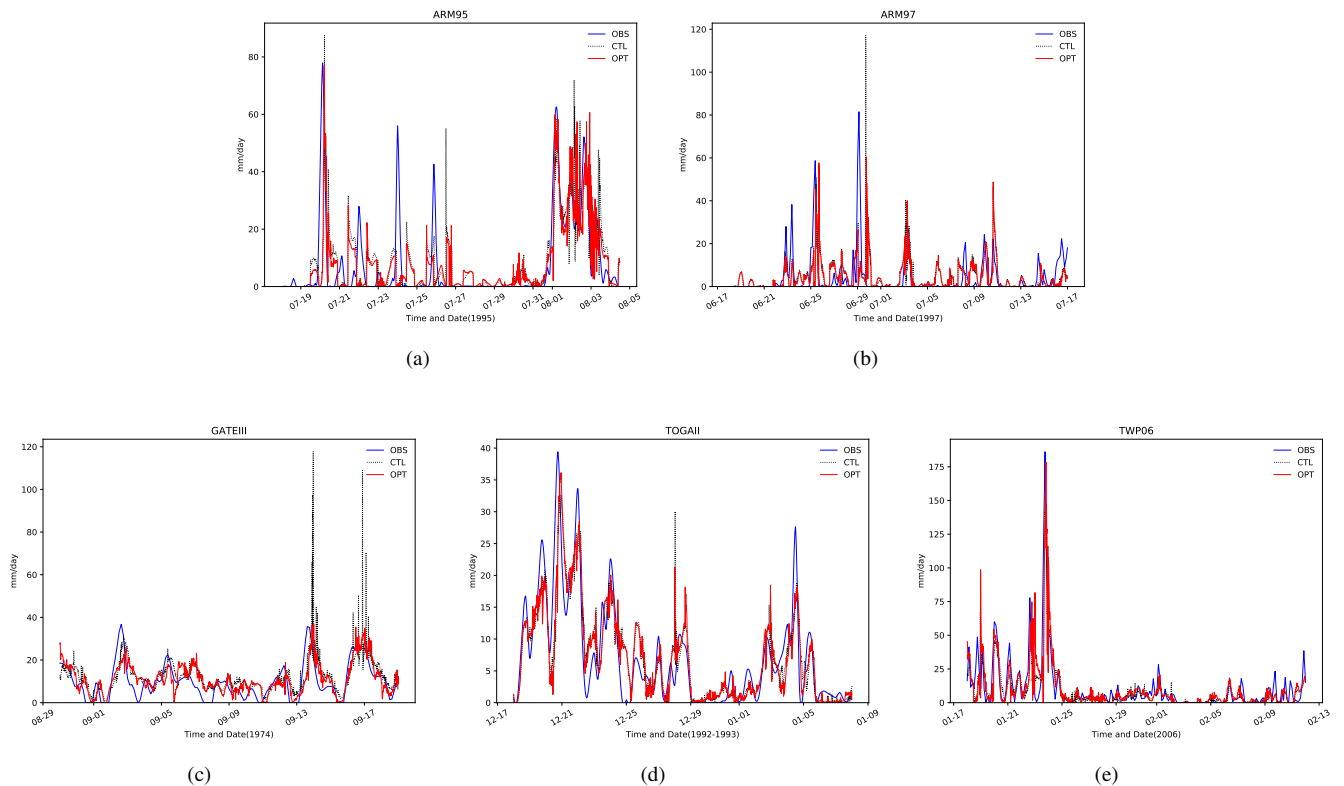
Figure 9. SCAM simulation output before and after tuning versus observed values in five cases. Where OBS indicates the observed value, CTL indicates the output before tuning and OPT indicates the output after tuning. (a)ARM95, (b)ARM97, (c)GATEIII, (d)TOGAII, (e)TWP06. It can be seen that the optimized output of each case is closer to the observation.

optimization, making it closer to the observation. This demonstrates the significance of the parameter tuning provided by our proposed LB-SCAM.

In contrast to using the optimization algorithm alone, the grid search combined with the optimization algorithm can achieve better results on these SCAM cases. The use of NN trained surrogate models for parameter tuning can further save computational resource overhead and, in terms of results, can meet or exceed traditional optimization methods in most cases.

In the previous sections, we mentioned that different sensitivity analysis methods yielded different conclusions for the output variable T850. Therefore, to demonstrate the performance differences among various methods, we decided to test the optimization results for different parameter combinations, as shown in Figure 10. Therefore, we can find that it is possible to achieve a win-win situation in terms of computational resources and computational efficiency by training a surrogate model of SCAM based on LB-SCAM.

After optimization, SCAM cases can get enhancement from 6.4%-24.4% in PRECT output, 11.9%-42.3% in Q850 output, 5.72%-22.4% in T850 output, and 3.8%-26.1% in CLDTOT output. Thus, using the proposed method, the main computational
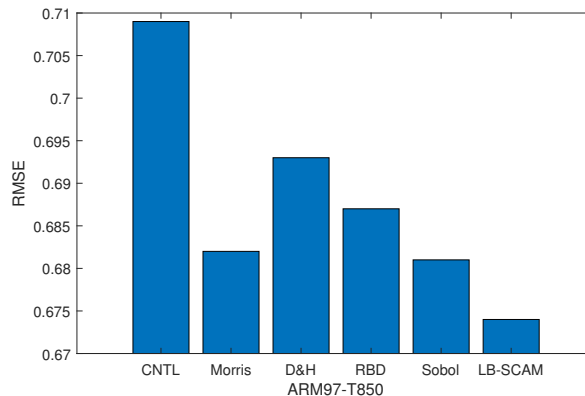
Figure 10. The optimized results of the sensitivity parameter combinations for the T850 output variable in the ARM97 case, as provided by various SA methods, are compared with the control experiment. D&H represents the common conclusions derived from the Delta and HDMR methods.

overhead comes from sampling and training. The computational overhead can be saved by more than 50% compared to the case where the above experiments are all run using the full SCAM. In particular, the proposed method demonstrates its effectiveness and usability for situations such as large-scale grid testing, which is almost impossible to accomplish using the full SCAM.

These results also show that the method used in the workflow outperforms previous methods in most cases. Furthermore, the methods in the workflow test a wide range of combinations of values in the parameter space. Thus using the workflow provides a more complete picture of the parametric characteristics of the different cases in SCAM than optimization algorithms that only provide results but no more information about the spatial distribution of the parameters. Doing a finer-grained grid search in the vicinity of the optimal value point is also an approach that is worth testing in the future. From the experimental results, it can be seen that utilizing the surrogate model through the sampling with the optimization algorithm not only saves resources, but also improves the optimization effect, and meanwhile improves the robustness of the optimization method.

4.6 A deeper exploration of the relationships between the cases for PRECT

The training of surrogate models makes it possible to conduct larger scale experiments in a shorter period of time. For the most sensitive combinations of parameters in each of the cases obtained based on the NN method, we are able to explore the distribution pattern of the results using a grid search. These experiments are carried out on the surrogate model for reasons of improving experimental efficiency.

Grid search can also be performed to determine the possible aggregation range of the better-valued solution. To make it easy to compare the same and different cases, we specify the same parameter space for each case. Based on the combined ranking of sensitive parameters under each case, we choose zmconv_tau, zmconv_alfa and cldfrc_rhminl as the parameter space common to all cases.The results are shown in Figure 11. The value of each parameter is also divided into 11 levels within its upper and lower bounds. The parameter space remains the same as originally set at the beginning of this paper.
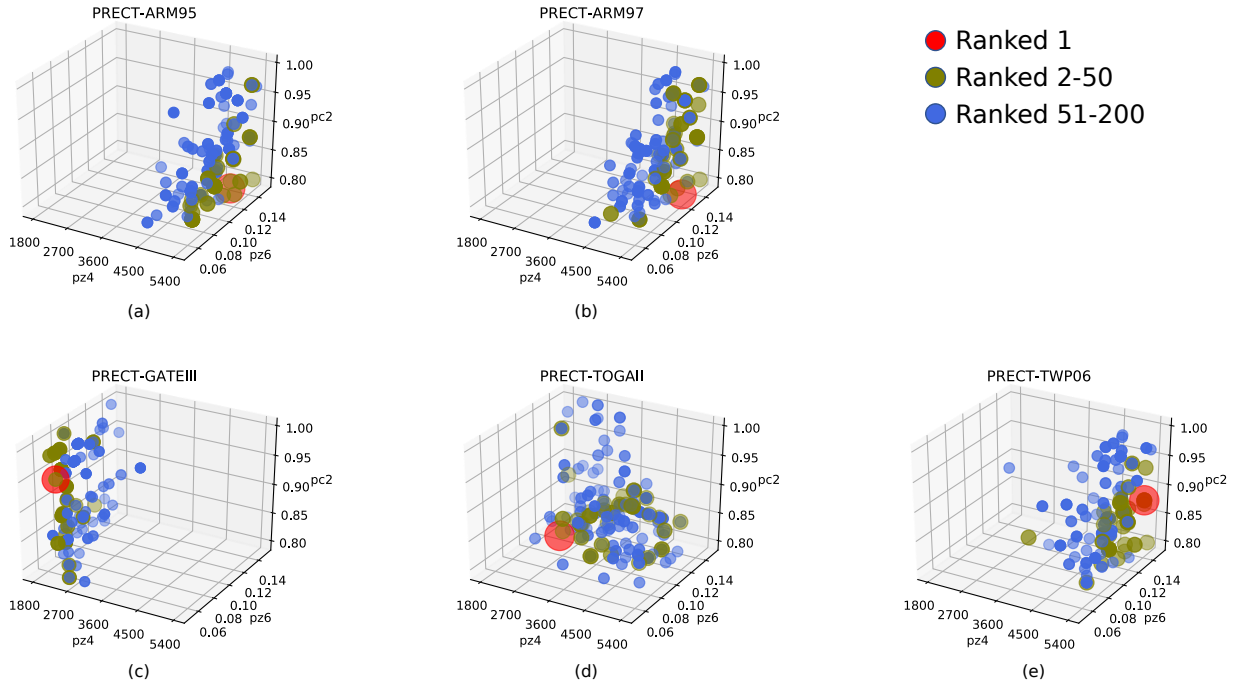
Figure 11. The distribution of better performing parameter solutions for PRECT in each case in the same 3D parameter space. (a)ARM95, (b)ARM97, (c)GATEIII, (d)TOGAII, (e)TWP06. The points closest to the observed data are shown in red, those ranked 2-50 are shown in olive, and those ranked 51-200 are shown in blue.

As can be seen, after the parameter space has been replaced, the better-valued solutions for each case show a clear trend towards aggregation, and although the distribution of TOGAII is slightly scattered, it can still be grouped into a cluster. The same parameter space is more conducive to cross-sectional comparisons. It is easy to see that the two land convection cases are closer, which matches our expectations since the two cases are themselves co-located. They have relatively high zmconv_tau and zmconv_alfa, and relatively lowest cldfrc_rhminl. For the three tropical convective cases, their distributions have their own characteristics. TWP06 has the highest tau and alfa, while TOGAII is in the middle for all parameters. The parametric response distributions of GATEIII are much more different. Its better performance relies on lower tau and alfa, and higher cldfrc_rhminl. As a site that is far away from all other cases, this also coincides with the previous results.

From the results, it can be seen that the distribution of the better values are different for different cases within the same parameter space. A typical example is the parameter zmconv_tau. This reflects the fact that it may be useful and necessary to adopt different parameter configurations for different cases or regions.

Now that we have discovered the pattern that the aggregation range of the more optimal solution for each case by applying a full-space grid search in the same parameter space. From the experimental results, it can be seen that the two cases focusing

on land convection are most similar to each other, and two of three cases focusing on tropical convection are also more similar
390   to each other, except for GATEIII.
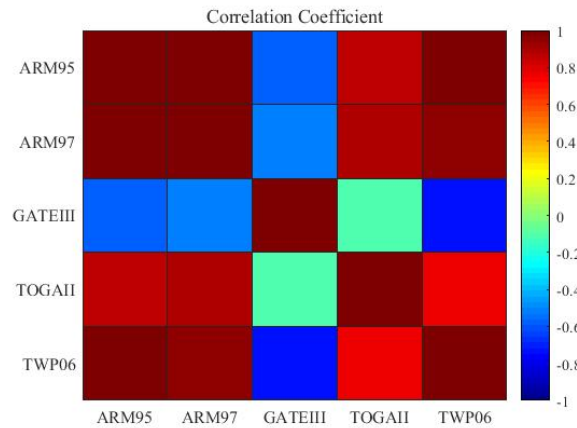
Figure 12. Correlation of the optimal solutions of PRECT for the cases in the same parameter space. The similarity difference between different cases can be seen.

Pearson correlation coefficient method is used to compare the best set of values for each case. The obtained similarity is shown in Figure 12. The average p-value in this experiment is less than 0.05, so it is relatively reliable. From this figure, we can see that the parameter values taken between the two cases of land convection are positively correlated in the same parameter space. The two of three cases of tropical convection, TOGAII and TWP06, are also positively correlated with each other.
395   The respective distributions of the above four cases are also positively correlated. The more special one is GATEIII, which is negatively correlated with the remaining four cases. These results are also well matched to those obtained in the previous experiments. It is also clear from the results above that SCAM cases in similar locations and of the same type are more relevant when it comes to parameterization.

5 Conclusions

400   In this paper, a learning-based integrated method for SCAM parameter tuning on the HPC is proposed which enables a fully automated diagnostic analysis process from sensitive tests to parameter optimization and case comparison. The workflow makes it possible to run SCAM parameters on a large scale, thus allowing more trials on parametric scenario studies to be carried out in a shorter period of time. An integration of several sensitivity methods approach is used for sensitivity analysis of parameters, with just once sampling, the different SA methods can be invoked for analysis and their results combined.
405   With the enhancement of artificial intelligence and machine learning techniques, the role played by neural networks in regression analysis has become increasingly evident. In our proposed experimental workflow, multiple regression methods including NNs incorporating sampling techniques are likewise used in the parametric analysis process of SCAM. A precursor

to sensitivity analysis: the results of the sampling are used to train an NN-based surrogate model, which validates the accuracy of both the sensitivity analysis and improves the parameter tuning process by the surrogate model. In these stages, a grid search strategy for parameter space based on multi-parameter perturbations is used. With the computational capabilities of the HPC, the method can search the most suitable parameter values within less iterations. The combination of grid search and optimization algorithms can also improves the performance of the optimization algorithm in model parameter tuning. In addition, the application of neural network-trained surrogate models can also saves computational resources, which is beneficial in achieving the goal of green computing.

To verify the completeness and validity of the proposed workflow, multi-group experiments based on five typical SCAM cases is implemented on the workflow. The sensitivity of the above parameters to typical output variables related to precipitation is analyzed. Experiments based on the proposed workflow have shown that there are differences in the sensitivities of the parameters with respect to the different cases and different output variables. This includes both the differences between the different convection types of cases and the differences in the effects of the deep and shallow convective precipitation parameterization schemes on the respective precipitation. To summarise, determining the appropriate values for each of the SCAM cases located at different locations facilitates is also meaningful for model development. This also provides a heuristic for future research on similar parametric schemes on other models.

Code and data availability. Open source code for this article is available at https://doi.org/10.6084/m9.figshare.21407109.v6 (Guo, 2023) along with the data used. The above is subject to the MIT License Agreement.

Author contributions. The manuscript was written by all authors. JG and HF proposed the main idea and method. JZ provides important guidance on neural networks. YX, WX and LW have provided important advice. JZ, PG and WW assisted in revising the manuscript. LH, GX and XC provided assistance and support with the experiments. XW and ZZ assisted in debugging the program. LG provides help with access to computing resources.

Competing interests. The authors declare that they have no conflict of interest.

Acknowledgements. This research was supported in part by the National Key Research and Development Plan of China (Grant No. 2020YFB0204800), National Natural Science Foundation of China (Grant No. T2125006, U1839206), Jiangsu Innovation Capacity Building Program (Project No. BM2022028), Project of Jilin Province Development and Reform Commission No. 2019FGWTZC001 and the Science and Technology Development Plan of Jilin Province of China under Grant 20220101115JC.

References

Bogenschutz, P. A., Gettelman, A., Morrison, H., Larson, V. E., Schanen, D. P., Meyer, N. R., and Craig, C.: Unified parameterization of the planetary boundary layer and shallow convection with a higher-order turbulence closure in the Community Atmosphere Model: Single-column experiments, Geoscientific Model Development, 5, 1407–1423, https://doi.org/10.5194/gmd-5-1407-2012, 2012.

Bogenschutz, P. A., Gettelman, A., Morrison, H., Larson, V. E., Craig, C., and Schanen, D. P.: Higher-Order Turbulence Closure and Its Impact on Climate Simulations in the Community Atmosphere Model, Journal of Climate, 26, 9655–9676, 2013.

Bogenschutz, P. A., Tang, S., Caldwell, P. M., Xie, S., Lin, W., and Chen, Y. S.: The E3SM version 1 single-column model, Geoscientific Model Development, 13, 4443–4458, https://doi.org/10.5194/gmd-13-4443-2020, 2020.

Breiman, L.: Random Forests, Machine Learning, 2001.

Caflisch, R. E.: Monte carlo and quasi-monte carlo methods, Acta numerica, 7, 1–49, 1998.

Dalbey, K. R., Eldred, M. S., Geraci, G., Jakeman, J. D., Maupin, K. A., Monschke, J. A., Seidl, D. T., Tran, A., Menhorn, F., and Zeng, X.: Dakota, A Multilevel Parallel Object-Oriented Framework for Design Optimization, Parameter Estimation, Uncertainty Quantification, and Sensitivity Analysis: Version 6.16 Theory Manual, https://doi.org/10.2172/1868423, 2021.

Fu, H., Liao, J., Yang, J., Wang, L., Song, Z., Huang, X., Yang, C., Xue, W., Liu, F., Qiao, F., Zhao, W., Yin, X., Hou, C., Zhang, C., Ge, W., Zhang, J., Wang, Y., Zhou, C., and Yang, G.: The Sunway TaihuLight supercomputer: system and applications, Science China Information Sciences, 59, https://doi.org/10.1007/s11432-016-5588-7, 2016.

Gettelman, A., Morrison, H., and Ghan, S. J.: A New Two-Moment Bulk Stratiform Cloud Microphysics Scheme in the Community Atmosphere Model, Version 3 (CAM3). Part II: Single-Column and Global Results, Journal of Climate, 21, 3660–3679, 2008.

Gettelman, A., Truesdale, J. E., Bacmeister, J. T., Caldwell, P. M., Neale, R. B., Bogenschutz, P. A., and Simpson, I. R.: The Single Column Atmosphere Model Version 6 (SCAM6): Not a Scam but a Tool for Model Evaluation and Development, Journal of Advances in Modeling Earth Systems, 11, 1381–1401, https://doi.org/10.1029/2018MS001578, 2019.

Goffart, J., Rabouille, M., and Mendes, N.: Uncertainty and sensitivity analysis applied to hygrothermal simulation of a brick building in a hot and humid climate, Journal of Building Performance Simulation, 10, 37–57, 2015.

Guo, J.: Learning-based_SCAM_Tuner, https://doi.org/10.6084/m9.figshare.21407109.v6, 2023.

Guo, Z., Wang, M., Qian, Y., Larson, V. E., Ghan, S., Ovchinnikov, M., Bogenschutz, P. A., Zhao, C., Lin, G., and Zhou, T.: A sensitivity analysis of cloud properties to CLUBB parameters in the Single Column Community Atmosphere Model (SCAM5), Journal of Advances in Modeling Earth Systems, 6, 829–858, 2015.

Harada, M.: GSA: Stata module to perform generalized sensitivity analysis, Statistical Software Components, 2012.

He, K., Zhang, X., Ren, S., and Sun, J.: Deep Residual Learning for Image Recognition, in: Proceedings of the IEEE Conference on Computer Vision and Pattern Recognition (CVPR), 2016.

Hurrell, J. W., Holland, M. M., Gent, P. R., Ghan, S., Kay, J. E., Kushner, P. J., Lamarque, J.-F., Large, W. G., Lawrence, D., Lindsay, K., Lipscomb, W. H., Long, M. C., Mahowald, N., Marsh, D. R., Neale, R. B., Rasch, P., Vavrus, S., Vertenstein, M., Bader, D., Collins, W. D., Hack, J. J., Kiehl, J., and Marshall, S.: The Community Earth System Model: A Framework for Collaborative Research, Bulletin of the American Meteorological Society, 94, 1339 – 1360, https://doi.org/10.1175/BAMS-D-12-00121.1, 2013.

Kennedy, J. and Eberhart, R.: Particle swarm optimization, in: Neural Networks, 1995. Proceedings., IEEE International Conference on, vol. 4, pp. 1942–1948, 2002.

Li, G., Rabitz, H., Yelvington, P. E., Oluwole, O. O., Bacon, F., Kolb, C. E., and Schoendorf, J.: Global Sensitivity Analysis for Systems with Independent and/or Correlated Inputs, Journal of Physical Chemistry A, 2, 7587–7589, 2010.

May, P. T., Mather, J. H., Vaughan, G., Bower, K. N., Jakob, C., Mcfarquhar, G. M., and Mace, G. G.: The tropical warm pool international cloud experiment, Bulletin of the American Meteorological Society, 89, 629–+, 2008.

McKay, M. D., Beckman, R. J., and Conover, W. J.: A comparison of three methods for selecting values of input variables in the analysis of output from a computer code, Technometrics, 42, 55–61, 2000.

Mirjalili, S. and Lewis, A.: The Whale Optimization Algorithm, Advances in Engineering Software, 95, 51–67, https://doi.org/10.1016/j.advengsoft.2016.01.008, 2016.

Mitchell, M.: An Introduction to Genetic Algorithms, 1996.

Morris, M. D.: Factorial sampling plans for preliminary computational experiments, Technometrics, 33, 161–174, https://doi.org/10.1080/00401706.1991.10484804, 1991.

Neale, R. B., Chen, C.-C., Gettelman, A., Lauritzen, P. H., Park, S., Williamson, D. L., Conley, A. J., Garcia, R., Kinnison, D., Lamarque, J.-F., et al.: Description of the NCAR community atmosphere model (CAM 5.0), NCAR Tech. Note NCAR/TN-486+ STR, 1, 1–12, 2010.

Nelder, J. A. and Wedderburn, R. W.: Generalized linear models, Journal of the Royal Statistical Society: Series A (General), 135, 370–384, 1972.

Park, S.: A Unified Convection Scheme (UNICON). Part I: Formulation, Journal of the Atmospheric Sciences, 71, 3902–3930, 2014.

Pathak, R., Dasari, H. P., El Mohtar, S., Subramanian, A. C., Sahany, S., Mishra, S. K., Knio, O., and Hoteit, I.: Uncertainty Quantification and Bayesian Inference of Cloud Parameterization in the NCAR Single Column Community Atmosphere Model (SCAM6), Frontiers in Climate, 3, https://doi.org/10.3389/fclim.2021.670740, 2021.

Plischke, E., Borgonovo, E., and Smith, C. L.: Global sensitivity measures from given data, European Journal of Operational Research, 226, 536–550, 2013.

Qian, Y., Yan, H., Hou, Z., Johannesson, G., Klein, S., Lucas, D., Neale, R., Rasch, P., Swiler, L., Tannahill, J., Wang, H., Wang, M., and Zhao, C.: Parametric sensitivity analysis of precipitation at global and local scales in the Community Atmosphere Model CAM5, Journal of Advances in Modeling Earth Systems, 7, 382–411, https://doi.org/https://doi.org/10.1002/2014MS000354, 2015.

Saltelli, A.: Making best use of model evaluations to compute sensitivity indices, Computer physics communications, 145, 280–297, 2002.

Saltelli, A., Ratto, M., Andres, T., Campolongo, F., Cariboni, J., Gatelli, D., Saisana, M., and Tarantola, S.: Global sensitivity analysis: the primer, John Wiley & Sons, 2008.

Saltelli, A., Annoni, P., Azzini, I., Campolongo, F., and Tarantola, S.: Variance based sensitivity analysis of model output. Design and estimator for the total sensitivity index, Computer Physics Communications, 181, 259–270, 2010.

Schober, P., Boer, C., and Schwarte, L. A.: Correlation Coefficients: Appropriate Use and Interpretation., Anesthesia & Analgesia, 126, 1763–1768, 2018.

Shi, L., Copot, C., and Vanlanduit, S.: Evaluating Dropout Placements in Bayesian Regression Resnet, Journal of Artificial Intelligence and Soft Computing Research, 12, 61–73, https://doi.org/10.2478/jaiscr-2022-0005, 2022.

Sobol', I. M.: On the distribution of points in a cube and the approximate evaluation of integrals, Zhurnal Vychislitel'noi Matematiki i Matematicheskoi Fiziki, 7, 784–802, 1967.

Sobol, I. M.: Sensitivity analysis for non-linear mathematical models, Mathematical modelling and computational experiment, 1, 407–414, 1993.

Storn, R. and Price, K.: Differential evolution–a simple and efficient heuristic for global optimization over continuous spaces, Journal of global optimization, 11, 341–359, 1997.

Tang, J., Deng, C., and Huang, G.-B.: Extreme Learning Machine for Multilayer Perceptron, IEEE TRANSACTIONS ON NEURAL NET-WORKS AND LEARNING SYSTEMS, 27, 809–821, https://doi.org/10.1109/TNNLS.2015.2424995, 2016.

Thompson, R. M., Payne, S. W., Recker, E., and Reed, R. J.: Structure and Properties of Synoptic-Scale Wave Disturbances in the Intertropical Convergence Zone of the Eastern Atlantic, J. Atmos., 36, 53–72, 1979.

Tong, C.: Problem Solving Environment for Uncertainty Analysis and Design Exploration, pp. 1–37, https://doi.org/10.1007/978-3-319-11259-6_53-1, 2016.

Webster, P. J. and Lukas, R.: TOGA COARE: the coupled ocean-atmosphere response experiment, Bulletin of the American Meteorological Society, 73, 1377–1416, 1992.

XingFen, W., Xiangbin, Y., and Yangchun, M.: Research on User Consumption Behavior Prediction Based on Improved XGBoost Algorithm, in: 2018 IEEE International Conference on Big Data (Big Data), pp. 4169–4175, IEEE, Seattle, WA, USA, ISBN 978-1-5386-5035-6, https://doi.org/10.1109/BigData.2018.8622235, 2018.

Yan, J., Chen, J., and Xu, J.: Analysis of Renting Office Information Based on Univariate Linear Regression Model, in: INTERNATIONAL CONFERENCE ON ELECTRICAL AND CONTROL ENGINEERING (ICECE 2015), pp. 780–784, Adv Sci Res Ctr, ISBN 978-1-60595-238-3, international Conference on Electrical and Control Engineering (ICECE), Guilin, PEOPLES R CHINA, APR 18-19, 2015, 2015.

Yang, B., Qian, Y., Lin, G., Leung, L. R., Rasch, P. J., Zhang, G. J., Mcfarlane, S. A., Zhao, C., Zhang, Y., and Wang, H.: Uncertainty quantification and parameter tuning in the CAM5 Zhang-McFarlane convection scheme and impact of improved convection on the global circulation and climate, Journal of Geophysical Research Atmospheres, 118, 395–415, 2013.

Zhang, G. J.: Sensitivity of climate simulation to the parameterization of cumulus convection in the Canadian Climate Centre general circulation model, Atmos. Ocean, 33, 1995.

Zhang, T., Zhang, M., Lin, W., Lin, Y., Xue, W., Yu, H., He, J., Xin, X., Ma, H. Y., Xie, S., and Zheng, W.: Automatic tuning of the Community Atmospheric Model (CAM5) by using short-term hindcasts with an improved downhill simplex optimization method, Geoscientific Model Development, 11, 5189–5201, https://doi.org/10.5194/gmd-11-5189-2018, 2018.

Zou, L., Qian, Y., Zhou, T., and Yang, B.: Parameter Tuning and Calibration of RegCM3 with MIT–Emanuel Cumulus Parameterization Scheme over CORDEX East Asia Domain, Journal of Climate, 27, 7687 – 7701, https://doi.org/https://doi.org/10.1175/JCLI-D-14-00229.1, 2014.